

Chih-Liang Chu

Yih-Hwang Lin

Department of Mechanical and  
Marine Engineering  
National Taiwan Ocean University  
Keelung City, Taiwan 20224  
Republic of China

---

# Finite Element Analysis of Fluid-Conveying Timoshenko Pipes

*A general finite element formulation using cubic Hermitian interpolation for dynamic analysis of pipes conveying fluid is presented. Both the effects of shearing deformations and rotary inertia are considered. The development retains the use of the classical four degrees-of-freedom for a two-node element. The effect of moving fluid is treated as external distributed forces on the support pipe and the fluid finite element matrices are derived from the virtual work done due to the fluid inertia forces. Finite element matrices for both the support pipe and moving fluid are derived and given explicitly. A numerical example is given to demonstrate the validity of the model. © 1995 John Wiley & Sons, Inc.*

---

## INTRODUCTION

The dynamic behavior of pipes transporting fluid has been a subject of increasing research interest. Païdoussis et al. (1976, 1986) examined the stability of tubes conveying fluid using global trial functions. To facilitate the analysis of more complex structures, such as pipes with intermediate supports, masses, and more general boundary conditions, Pramila and Laukkanen (1991) applied a finite element formulation by using linear shape functions to independently interpolate the displacements and rotations of a Timoshenko beam element. Because the element used experiences severe problems for thin beams, known as shear locking, reduced integration by employing one point quadrature must be used to improve the accuracy (Hughes et al., 1977).

It has been demonstrated that for static analysis considering shear effect, the element using consistent interpolation with quadratic approxi-

mation of displacement and linear approximation of rotation yields more accurate results than the element with linear shape functions with reduced integration, due to better representation of the load (Reddy, 1993). To further improve the analysis accuracy, cubic approximation of displacement can be considered. Such an element was developed by Narayanaswami and Adelman in 1974 for static analysis including shear effect without using additional nodal degrees-of-freedom; three additional degrees-of-freedom are required to control transverse shear for the element developed by Nickell and Secor (1972). The purpose of this study is to extend this more accurate formulation developed by Narayanaswami and Adelman (1974), with the classical formulation of two-node element with four degrees-of-freedom still retained. Both the effects of shearing deformations and rotary inertia are considered for dynamic analysis of pipes conveying fluid.

---

Received September 21, 1994; Accepted January 3, 1995.

Shock and Vibration, Vol. 2, No. 3, pp. 247–255 (1995)  
© 1995 John Wiley & Sons, Inc.

CCC 1070-9622/95/030247-09

After completion of this work we were aware of a somewhat similar study by Stack et al. (1993), where the standard form of Hamiltonian principle was applied to derive the equations of motion, and an interesting analysis of the dynamic behavior of Coriolis mass flow meters was conducted. However, the analysis is limited to fluid-conveying pipes with supported ends. When one end of the pipe is free, the extended Hamiltonian principle must be used to take into account the outflow dynamics (McIver, 1973). Note that the Coriolis matrix is incorrectly given in Stack's paper. All  $v_0^2$  terms should be replaced with  $v_0$  and the sign of  $b_{21}$  should be negative. In this article the effect of the moving fluid is taken as external loads acting on the pipe, without differentiating whether the loads are conservative or nonconservative. The laborious derivation using the variational principle is avoided by considering the virtual work done by the fluid inertia forces. This analysis includes the outflow dynamics so that pipes with free ends can be correctly analyzed. Explicit beam and moving fluid element matrices will be given to facilitate design and analysis applications. The validity of this work will be verified by comparing the analysis results with those obtained by Paidoussis et al. (1986).

## MODEL DEVELOPMENT

The finite element model for both the support pipe and the moving fluid is presented in this section. This development will include analyses for both the Timoshenko and Bernoulli-Euler pipes.

### Timoshenko Pipe Element

Narayanaswami and Adelman (1974) reported a straightforward energy minimization approach for static analysis of beam structures considering the shear effect. Correct formulation of the finite element characteristics was obtained without using additional nodal degrees-of-freedom. A traditional cubic polynomial can still be used to describe the transverse displacement. The shear strain within an element is described as

$$\gamma = \frac{\partial w}{\partial x} - \theta \quad (1)$$

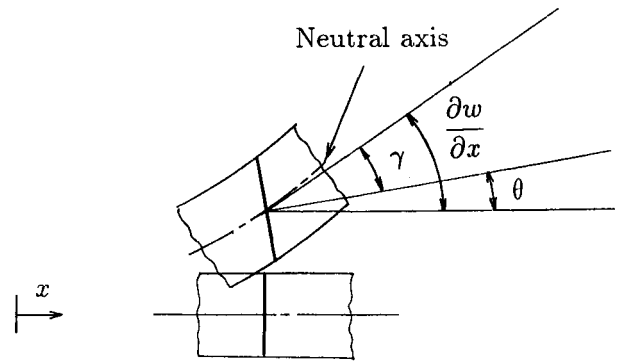


FIGURE 1 Deformation of the cross section considering shear effect

where  $w$  denotes transverse displacement of the pipe,  $\theta$  the cross-section rotation, and  $\gamma$  the shear strain. Figure 1 illustrates the deformation of the cross section considering the shear effect. The transverse displacement and rotation of the pipe are interpolated as

$$w = [N] \{d\}_e, \quad \theta = [\bar{N}] \{d\}_e \quad (2)$$

where  $[N]$  and  $[\bar{N}]$  denote  $1 \times 4$  row vectors representing shape functions,  $\{d\}_e$  the element nodal degrees-of-freedom vector including transverse displacements and rotations.

The following shape functions for both the transverse displacement and cross-section rotation can be obtained with the Hermitian interpolation being used to describe the transverse displacement of the pipe.

$$\begin{aligned} N_1 &= 1 - \frac{1}{a(a^2 + 12g)} (12gx + 3ax^2 - 2x^3) \\ N_2 &= \frac{1}{a(a^2 + 12g)} [(a^2 + 6g)ax \\ &\quad - (2a^2 + 6g)x^2 + ax^3] \\ N_3 &= \frac{1}{a(a^2 + 12g)} (12gx + 3ax^2 - 2x^3) \\ N_4 &= \frac{1}{a(a^2 + 12g)} [-6gax \\ &\quad + (6g - a^2)x^2 + ax^3] \end{aligned} \quad (3)$$

and

$$\begin{aligned}\bar{N}_1 &= \frac{1}{a(a^2 + 12g)} (6x^2 - 6ax) \\ \bar{N}_2 &= \frac{1}{a(a^2 + 12g)} [a^3 + 12ga \\ &\quad - (4a^2 + 12g)x + 3ax^2] \\ \bar{N}_3 &= \frac{1}{a(a^2 + 12g)} (6ax - 6x^2) \\ \bar{N}_4 &= \frac{1}{a(a^2 + 12g)} [3ax^2 \\ &\quad - (2a^2 - 12g)x]\end{aligned}\quad (4)$$

where

$$g = \frac{EI}{kGA} \quad (5)$$

and  $a$  is the beam element length,  $EI$  the bending rigidity,  $k$  the shear coefficient,  $G$  the shear modulus,  $A$  the cross-section area of the pipe element, and  $x$  the coordinate along the longitudinal direction of the pipe element. For pipes with circular cross section, the shear coefficient derived by Cowper (1966) by integrating the three-dimensional elasticity equations was used here:

$$k = \frac{6(1 + \nu)(1 + m^2)^2}{(7 + 6\nu)(1 + m^2)^2 + (20 + 12\nu)m^2} \quad (5a)$$

where  $\nu$  is the Poisson ratio and  $m$  the ratio of the inside diameter to the outside diameter. The strain energy including the shear effect for a pipe element of length,  $a$ , can be described as

$$U_e = \frac{1}{2} \int_0^a EI \left( \frac{\partial \theta}{\partial x} \right)^2 dx + \frac{1}{2} \int_0^a kGA \gamma^2 dx. \quad (6)$$

The stiffness matrix can be obtained directly from the description of strain energy by substituting Eqs. (1) and (2) into Eq. (6).

$$[k]_e = [k_b]_e + [k_s]_e \quad (7)$$

where

$$[k_b]_e = \int_0^a EI [\bar{N}_x]^T [\bar{N}_x] dx \quad (8)$$

represents the bending effect, and

$$[k_s]_e = \int_0^a kGA ([N_x]^T - [\bar{N}]^T) ([N_x] - [\bar{N}]) dx \quad (9)$$

describes the shear effect. The subscript  $x$  associated with the shape functions denotes differentiation. Thus

$$[k]_e = \frac{12}{(a^2 + 12g)} \frac{EI}{a} \begin{bmatrix} 1 & & & \text{sym} \\ \frac{a}{2} & \frac{a^2}{3} + g & & \\ -1 & -\frac{a}{2} & 1 & \\ \frac{a}{2} & \frac{a^2}{6} - g & -\frac{a}{2} & \frac{a^2}{3} + g \end{bmatrix} \quad (10)$$

which is the pipe element stiffness matrix including the traditional bending effect with the addition of shear effect. Note that if  $g$  is zero, which represents an infinite shear rigidity, the matrix reduces to the classical element stiffness matrix using Bernoulli-Euler's beam theory.

Equation (10) was available in the work by Narayanaswami and Adelman (1974), in which the static analysis of short beams considering the effect of shearing deformations was presented. For dynamic analysis of a short pipe, considering both the effects of shearing deformations and rotary inertia, the mass matrix including these effects needs to be determined in addition to the previous development.

The kinetic energy of the pipe can be written as

$$T_e = \frac{1}{2} \int_0^a \rho A \left( \frac{\partial w}{\partial t} \right)^2 dx + \frac{1}{2} \int_0^a \rho I \left( \frac{\partial \theta}{\partial t} \right)^2 dx \quad (11)$$

where  $\rho$  is the mass density per unit volume of the pipe. Substituting the shape functions and knowing that they are functions of  $x$  only, the pipe element mass matrix,  $[m]_e$ , can be described as

$$[m]_e = [m_t]_e + [m_r]_e \quad (12)$$

in which  $[m_t]_e$  is the mass matrix for an element due to the translational inertia and can be shown to be

$$[m_t]_e = \int_0^a [N]^T \rho A [N] dx \quad (13a)$$

therefore

$$[m_t]_e = \frac{\rho A a}{(a^2 + 12g)^2} \begin{bmatrix} t_{11} & & & \text{sym} \\ t_{21} & t_{22} & & \\ t_{31} & t_{32} & t_{33} & \\ t_{41} & t_{42} & t_{43} & t_{44} \end{bmatrix} \quad (13b)$$

where

$$\begin{aligned} t_{11} &= \frac{13}{35} a^4 + \frac{42}{5} g a^2 + 48 g^2 \\ t_{21} &= \left( \frac{11}{210} a^4 + \frac{11}{10} g a^2 + 6 g^2 \right) a \\ t_{22} &= \left( \frac{1}{105} a^4 + \frac{1}{5} g a^2 + \frac{6}{5} g^2 \right) a^2 \\ t_{31} &= \frac{9}{70} a^4 + \frac{18}{5} g a^2 + 24 g^2 \\ t_{32} &= \left( \frac{13}{420} a^4 + \frac{9}{10} g a^2 + 6 g^2 \right) a \\ t_{33} &= t_{11} \\ t_{41} &= -t_{32} \\ t_{42} &= -\left( \frac{1}{140} a^4 + \frac{1}{5} g a^2 + \frac{6}{5} g^2 \right) a^2 \\ t_{43} &= -t_{21} \\ t_{44} &= t_{22} \end{aligned} \quad (13c)$$

and  $[m_r]_e$  is the element mass matrix denoting the contribution due to rotary inertia:

$$[m_r]_e = \int_0^a [\bar{N}]^T \rho I [\bar{N}] dx \quad (14a)$$

thus

$$[m_r]_e = \frac{\rho A a}{(a^2 + 12g)^2} \left( \frac{r}{a} \right)^2 \begin{bmatrix} r_{11} & & & \text{sym} \\ r_{21} & r_{22} & & \\ r_{31} & r_{32} & r_{33} & \\ r_{41} & r_{42} & r_{43} & r_{44} \end{bmatrix} \quad (14b)$$

where

$$\begin{aligned} r_{11} &= \frac{6}{5} a^4 \\ r_{21} &= \left( \frac{1}{10} a^2 - 6g \right) a^3 \\ r_{22} &= \left( \frac{2}{15} a^4 + 2ga^2 + 48g^2 \right) a^2 \\ r_{31} &= -r_{11} \\ r_{32} &= -r_{21} \\ r_{33} &= r_{11} \\ r_{41} &= r_{21} \\ r_{42} &= \left( -\frac{1}{30} a^4 - 2ga^2 + 24g^2 \right) a^2 \\ r_{43} &= -r_{21} \\ r_{44} &= r_{22} \end{aligned} \quad (14c)$$

where  $r$  is the radius of gyration of the pipe cross section. The above element mass and stiffness matrices can be assembled to form the pipe structural matrices. Note that when pipe damping is considered, Rayleigh damping of the type,  $[C] = \alpha[M] + \beta[K]$ , can be used to form the pipe structural damping matrix. The constants,  $\alpha$  and  $\beta$ , can be determined from the modal dampings obtained using the experimental modal analysis technique (Ewins, 1986). When more than two modal dampings need to be accurately represented, a Caughey series can be applied to form the damping matrix (Bathe, 1982).

### Moving Fluid Model

The development of the fluid finite element model for a Timoshenko or Bernoulli-Euler pipe conveying fluid is described in this section. By denoting the coordinate of the fluid as  $w_0(x, t)$  and that of the support beam as  $w(x, t)$  and knowing that they are the same at the contact position, the time derivatives of  $w_0$  can be described as

$$\begin{aligned} \dot{w}_0(x, t) &= w_{xx} \dot{x}^2 + 2w_{xt} \dot{x} + w_x \ddot{x} + w_{tt} \\ &= w_{xx} v^2 + 2w_{xt} v + w_x \dot{v} + w_{tt} \end{aligned} \quad (15)$$

in which a subscript denotes partial differentiation, and  $v$  is the fluid flow velocity with its overdot denoting the acceleration. From Eq. (2), the following relationship can be established

$$\begin{aligned} w_{xx} &= [N]_{xx}\{d\}; & w_{xt} &= [N]_x\{\dot{d}\} \\ w_x &= [N]_x\{d\}; & w_{tt} &= [N]\{\ddot{d}\}. \end{aligned} \quad (16)$$

In this article the effects of moving fluid are treated as external forces on the support pipe, and the forces turn out to be dependent on the system nodal variables. Equations (15) and (16) can be combined and integrated over the element span to obtain the fluid element mass, damping, and stiffness matrices for the moving fluid by considering the virtual work done by the fluid inertia forces

$$\delta W_e = - \int_0^a p \delta w dx \quad (17a)$$

where  $p$  denotes all fluid inertia forces. Note that there is no need to differentiate the conservative and nonconservative fluid inertia forces, as stated by Dupuis and Rousselet (1992), for correct derivation. Thus,

$$\begin{aligned} [m_f]_e &= \mu_f \int_0^a [N]^T [N] dx + \rho_f I_f \int_0^a [\bar{N}]^T [\bar{N}] dx \\ [c_f]_e &= 2\mu_f v \int_0^a [N]^T [N]_x dx - \mu_f v [N]^T [N] \Big|_{x=0}^{x=a} \\ [k_f]_e &= \mu_f v^2 \int_0^a [N]^T [N]_{xx} dx + \mu_f \dot{v} \int_0^a [N]^T [N]_x dx \\ &\quad - \mu_f v^2 [N]^T [N]_x \Big|_{x=0}^{x=a} \end{aligned} \quad (17b)$$

where  $\mu_f$  is the mass per unit length of the fluid. The last terms in the right-hand-side of the damping and stiffness matrices expressions, which are not attributed to Eq. (17a), represent the inflow at  $x = 0$ , and outflow at  $x = a$ , as the fluid enters the pipe element from one end and exits from the other to account for the fluid boundary conditions (McIver, 1973). The above finite element matrices for both the pipe and the moving fluid can be assembled to form the structural matrices for analysis. Note that at the free end of the pipe, the outflow terms as depicted above need to be added to the structural matrices for correct formulation. For a cantilever pipe with its right end unsupported, the outflow terms are explicitly shown as:

$$\mu_f v [N]^T [N] \Big|_{x=a} = \mu_f v \begin{bmatrix} 0 & & & \text{sym} \\ 0 & 0 & & \\ 0 & 0 & 1 & \\ 0 & 0 & 0 & 0 \end{bmatrix} \quad (17c)$$

and

$$\begin{aligned} \mu_f v^2 [N]^T [N]_x \Big|_{x=a} &= \frac{\mu_f v^2}{a(a^2 + 12g)} \\ &\begin{bmatrix} 0 & 0 & 0 & 0 \\ 0 & 0 & 0 & 0 \\ -12g & -6ag & 12g & a^3 + 6ag \\ 0 & 0 & 0 & 0 \end{bmatrix}. \end{aligned} \quad (17d)$$

### Fluid Model for Timoshenko Pipe Support

The fluid element mass matrix can be written as

$$[m_f]_e = [m_n]_e + [m_{fr}]_e \quad (18)$$

where  $[m_n]_e$  denotes the translational inertia effect of the moving fluid

$$[m_n]_e = \mu_f \int_0^a [N]^T [N] dx, \quad (19a)$$

thus

$$[m_n]_e = \frac{\mu_f a}{(a^2 + 12g)^2} \begin{bmatrix} ft_{11} & & & \text{sym} \\ ft_{21} & ft_{22} & & \\ ft_{31} & ft_{32} & ft_{33} & \\ ft_{41} & ft_{42} & ft_{43} & ft_{44} \end{bmatrix} \quad (19b)$$

where

$$\begin{aligned} ft_{11} &= \frac{13}{35} a^4 + \frac{42}{5} ga^2 + 48g^2 \\ ft_{21} &= \left( \frac{11}{210} a^4 + \frac{11}{10} ga^2 + 6g^2 \right) a \\ ft_{22} &= \left( \frac{1}{105} a^4 + \frac{1}{5} ga^2 + \frac{6}{5} g^2 \right) a^2 \\ ft_{31} &= \frac{9}{70} a^4 + \frac{18}{5} ga^2 + 24g^2 \\ ft_{32} &= \left( \frac{13}{420} a^4 + \frac{9}{10} ga^2 + 6g^2 \right) a \end{aligned} \quad (19c)$$

$$\begin{aligned}
ft_{33} &= ft_{11} \\
ft_{41} &= -ft_{32} \\
ft_{42} &= -\left(\frac{1}{140}a^4 + \frac{1}{5}ga^2 + \frac{6}{5}g^2\right)a^2 \\
ft_{43} &= -ft_{21} \\
ft_{44} &= ft_{22}
\end{aligned}$$

and  $[m_{fr}]_e$  describes the fluid rotary inertia effect

$$[m_{fr}]_e = \rho_f I_f \int_0^a [\bar{N}]^T [\bar{N}] dx, \quad (20a)$$

thus

$$[m_{fr}]_e = \rho_f I_f \begin{bmatrix} fr_{11} & & & \text{sym} \\ fr_{21} & fr_{22} & & \\ fr_{31} & fr_{32} & fr_{33} & \\ fr_{41} & fr_{42} & fr_{43} & fr_{44} \end{bmatrix} \quad (20b)$$

where

$$\begin{aligned}
fr_{11} &= \frac{6a^3}{5(a^2 + 12g)^2} \\
fr_{21} &= \frac{a^4 - 60a^2g}{10(a^2 + 12g)^2} \\
fr_{22} &= \frac{2a^5 + 30a^3g + 720ag^2}{15(a^2 + 12g)^2} \\
fr_{31} &= -fr_{11} \\
fr_{32} &= -fr_{21} \\
fr_{33} &= fr_{11} \\
fr_{41} &= fr_{21} \\
fr_{42} &= \frac{-a^5 - 60a^3g + 720ag^2}{30(a^2 + 12g)^2} \\
fr_{43} &= -fr_{21} \\
fr_{44} &= fr_{22}
\end{aligned} \quad (20c)$$

The fluid element damping matrix, known as gyroscopic matrix, is shown below

$$[c_f]_e = \frac{\mu_f v}{30(a^2 + 12g)} \begin{bmatrix} 0 & & & \\ -6(a^3 + 10ag) & & & \\ -30(a^2 + 12g) & & & \\ 6(a^3 + 10ag) & & & \\ 6(a^3 + 10ag) & 30(a^2 + 12g) & -6(a^3 + 10ag) & \\ 0 & 6(a^3 + 10ag) & -a^4 & \\ -6(a^3 + 10ag) & 0 & 6(a^3 + 10ag) & \\ a^4 & -6(a^3 + 10ag) & 0 & \end{bmatrix}. \quad (21)$$

Note that the fluid damping matrix is skew symmetric. The fluid element stiffness matrix is

$$[k_f]_e = [k_v]_e + [k_a]_e \quad (22)$$

where

$$[k_v]_e = \frac{-\mu_f v^2}{60a(a^2 + 12g)^2} \begin{bmatrix} kv_{11} & & & \text{sym} \\ kv_{21} & kv_{22} & & \\ kv_{31} & kv_{32} & kv_{33} & \\ kv_{41} & kv_{42} & kv_{43} & kv_{44} \end{bmatrix} \quad (23a)$$

in which

$$\begin{aligned}
kv_{11} &= 72(a^4 + 20a^2g + 120g^2) \\
kv_{21} &= 6a^5 \\
kv_{22} &= 8(a^6 + 15a^4g + 90a^2g^2) \\
kv_{31} &= -kv_{11} \\
kv_{32} &= -kv_{21} \\
kv_{33} &= kv_{11} \\
kv_{41} &= kv_{21} \\
kv_{42} &= -2(a^6 + 60a^4g + 360a^2g^2) \\
kv_{43} &= -kv_{21} \\
kv_{44} &= kv_{22}
\end{aligned} \quad (23b)$$

and the matrix for the effect of fluid acceleration is

$$[k_a]_e = \frac{\mu_f \dot{v}}{60(a^2 + 12g)} \begin{bmatrix} -30(a^2 + 12g) & & & \\ -6(a^3 + 10ag) & & & \\ -30(a^2 + 12g) & & & \\ 6(a^3 + 10ag) & & & \end{bmatrix} \\ + \frac{\mu_f \dot{v}}{60} \begin{bmatrix} 6(a^3 + 10ag) & 30(a^2 + 12g) & -6(a^3 + 10ag) & \\ 0 & 6(a^3 + 10ag) & -a^4 & \\ -6(a^3 + 10ag) & 30(a^2 + 12g) & 6(a^3 + 10ag) & \\ a^4 & -6(a^3 + 10ag) & 0 & \end{bmatrix} \quad (24)$$

### Fluid Model for Bernoulli–Euler Pipe Support

For analysis of a Bernoulli–Euler pipe conveying fluid, the entries in the above element matrices are replaced by expressions shown below, using the ordinary shape function rather than that depicted in Eq. (3). The fluid element mass, damping, and stiffness matrices can be shown to be

$$[m_f]_e = \frac{\mu_f a}{420} \begin{bmatrix} 156 & & & & \text{sym} \\ 22a & 4a^2 & & & \\ 54 & 13a & 156 & & \\ -13a & -3a^2 & -22a & 4a^2 & \end{bmatrix} \quad (25)$$

for the moving fluid element mass matrix,

$$[c_f]_e = \frac{\mu_f v}{30} \begin{bmatrix} 0 & 6a & 30 & -6a \\ -6a & 0 & 6a & -a^2 \\ -30 & -6a & 0 & 6a \\ 6a & a^2 & -6a & 0 \end{bmatrix} \quad (26)$$

for the moving fluid element damping matrix, and

$$[k_f]_e = \frac{\mu_f v^2}{30a} \begin{bmatrix} -36 & & & & \text{sym} \\ -3a & -4a^2 & & & \\ 36 & 3a & -36 & & \\ -3a & a^2 & 3a & -4a^2 & \end{bmatrix} \\ + \frac{\mu_f \dot{v}}{60} \begin{bmatrix} -30 & 6a & 30 & -6a \\ -6a & 0 & 6a & -a^2 \\ -30 & -6a & 30 & 6a \\ 6a & a^2 & -6a & 0 \end{bmatrix} \quad (27)$$

for the moving fluid element stiffness matrix.

### MODEL EVALUATION

The Timoshenko pipe/fluid element presented in this work was numerically implemented to examine the dynamic characteristics of a fluid-conveying cantilever pipe with flow exiting from the free end. For a cantilever pipe the system is nonconservative and the Coriolis fluid forces do work for the system. When the flow velocity is low, the effect of fluid flow decreases the eigenfrequencies and introduces fluid damping to the system. However, when the flow velocity increases, the Coriolis damping effect reaches a maximum and then diminishes. At sufficiently high flow velocity, the total effective damping vanishes and the cantilever pipe loses stability by flutter. Apparently the dynamic behavior of cantilever pipes conveying fluid is more complex than that of pipes with both ends supported, where the system can never lose stability by flutter (Holmes, 1978).

The following dimensionless parameters are used in the present analysis:

$$\beta = \frac{\mu_f}{\mu_f + \rho A}, \quad U_{cr} = \left( \frac{\mu_f}{EI} \right)^{1/2} u_{cr} L \quad (28)$$

$$\Omega = \left( \frac{(\mu_f + \rho A)L^4}{EI} \right)^{1/2} \omega, \quad \Lambda = \frac{kGAL^2}{EI} \quad (29)$$

where  $L$  is the total pipe length and  $u_{cr}$  is the critical fluid moving speed for the fluid-conveying pipe to become unstable. The parameter  $\Lambda$  is a measure of how slender the pipe is and hence

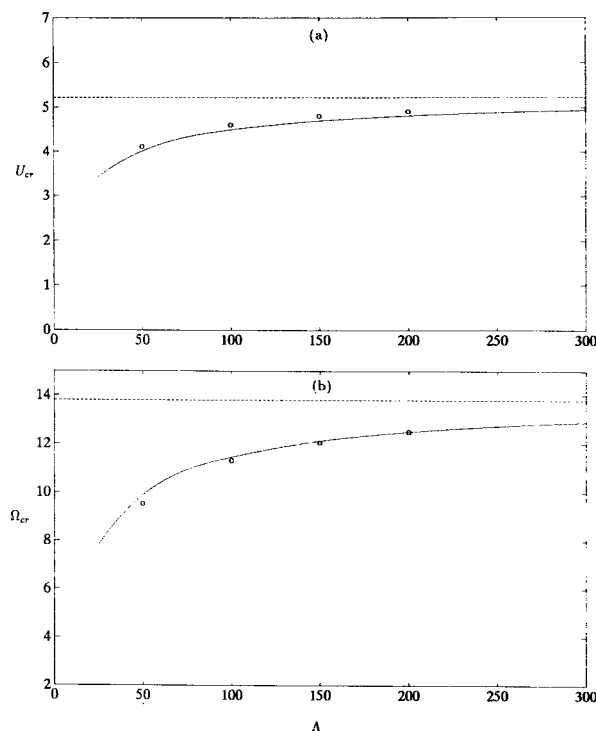


**FIGURE 2** Nondimensional (a) critical velocity and (b) the corresponding angular frequency as a function of the slenderness ratio. (---) Bernoulli-Euler element; (—) Timoshenko element (this work); (O) Timoshenko theory (Païdoussis et al., 1986).

for higher  $\Lambda$ , the analysis results using the Timoshenko beam theory are expected to approach those using the Bernoulli-Euler beam theory, because the effects of shearing deformation and rotary inertia are insignificant for long slender pipes. The first two modal damping ratios used to construct the structural damping matrix are  $\zeta_1 = \zeta_2 = 0.01$  and the mass ratio  $\beta$  is 0.155.

Figure 2 shows the nondimensional critical velocity  $U_{cr}$  and the corresponding nondimensional angular frequency  $\Omega_{cr}$  as a function of the slenderness ratio  $\Lambda$ . If the pipe becomes shorter, corresponding to lower  $\Lambda$ , the nondimensional critical velocity  $U_{cr}$  and the corresponding nondimensional angular frequency  $\Omega_{cr}$  are smaller, and the classical Bernoulli-Euler's beam theory gives identical results independent of the slenderness ratio. This is in accordance with the fact that the Timoshenko beam theory, considering both the effects of shearing deformations and rotary inertia, gives a more realistic and accurate representation of short pipes by releasing the constraints of infinite shear rigidity

and zero rotary inertia as made in the Bernoulli-Euler beam theory. This release of inappropriate constraints for a short pipe makes the structure less rigid, in addition to having more inertia effect, hence the moving fluid speed required to make the system unstable becomes smaller and the corresponding frequency of oscillation is decreased. As can be seen in Figure 2, the numerical results obtained here are in good agreement with those given by Païdoussis et al. (1986) that have been verified experimentally.

## CONCLUSIONS

A general finite element formulation using cubic Hermitian interpolation has been presented to describe the dynamic behavior of pipes conveying fluid. Both the Timoshenko and Bernoulli-Euler theories are included in the development. The use of this finite element scheme provides accurate dynamic analysis for complicated systems such as structures with nonuniform cross section, complex boundary conditions, intermediate supports and masses, etc. Classical analytical approach may be quite difficult to apply in dealing with these complex practical systems. Explicit element matrices have been provided to facilitate design and analysis.

The authors are grateful to the National Science Council (NSC), Republic of China, for the financial support under Grant No. NSC 81-0403-E-019-514.

## REFERENCES

- Bathe, K. J., 1982, *Finite Element Procedures in Engineering Analysis*, Prentice-Hall, Inc., Englewood Cliffs, NJ.
- Cowper, G. R., 1966, "The Shear Coefficient in Timoshenko's Beam Theory," *Transactions of the ASME Journal of Applied Mechanics*, Vol. 33, pp. 335-340.
- Dupuis, C., and Rousselet, J., 1992, Discussion on "Dynamics and Stability of Short Fluid-conveying Timoshenko Element Pipes," *Journal of Sound and Vibrations*, Vol. 152(3), pp. 561-563.
- Ewins, D. J., 1986, *Modal Testing: Theory and Practice*, Research Studies Press Ltd, Hertfordshire, England.
- Holmes, P. J., 1978, "Pipes Supported at Both Ends Cannot Flutter," *Transactions of the ASME Journal of Applied Mechanics*, Vol. 45, pp. 619-622.



- Hughes, T. J. R., Taylor, R. L., and Kanoknukulchai, W., 1977, "A Simple and Efficient Finite Element for Plate Bending," *International Journal for Numerical Methods in Engineering*, Vol. 11, pp. 1529–1543.
- McIver, D. B., 1973, "Hamilton's Principle for Systems of Changing Mass," *Journal of Engineering Mathematics*, Vol. 73, pp. 249–261.
- Narayanaswami, R., and Adelman, H. M., 1974, "Inclusion of Transverse Shear Deformation in Finite Element Displacement Formulation," *AIAA Journal*, Vol. 12(11), pp. 1613–1614.
- Nickell, R. E., and Secor, G. A., 1972, "Convergence of Consistently Derived Timoshenko Beam Finite Element," *International Journal for Numerical Methods in Engineering*, Vol. 5, pp. 243–253.
- Païdoussis, M. P., and Laithier, B. E., 1976, "Dynamics of Timoshenko Beams Conveying Fluid," *Journal of Mechanical Engineering Science*, Vol. 18, pp. 210–220.
- Païdoussis, M. P., Luu, T. P., and Laithier, B. E., 1986, "Dynamics of Finite Length Tubular Beams Conveying Fluid," *Journal of Sound and Vibration*, Vol. 106, pp. 311–331.
- Pramila, A., and Laukkanen, J., 1991, "Dynamics and Stability of Short Fluid-Conveying Timoshenko Element Pipes," *Journal of Sound and Vibration*, Vol. 144(3), pp. 421–425.
- Reddy, J. N., 1993, *An Introduction to the Finite Element Method*, McGraw-Hill, Inc., New York.
- Stack, C. P., Garnett, R. B., and Pawlas, G. E., 1993, "A Finite Element for the Vibration Analysis of a Fluid-Conveying Timoshenko Beam," *Proceedings of the 34th AIAA/ASCE/AHS/ASC Conference on Structures, Structural Dynamics and Materials*, pp. 2120–2129.

